



**HAL**  
open science

## Geometry, Extent, and Chemistry of Fermentative Hot Spots in Municipal Waste Souk Sebt Landfill, Ouled Nemma, Beni Mellal, Morocco

Yousra El Mouine, Amal El Hamdi, Abderrahim Bousouis, Youssouf El Jarjini, Meryem Touzani, Vincent Valles, Laurent Barbiero, Moad Morarech

► **To cite this version:**

Yousra El Mouine, Amal El Hamdi, Abderrahim Bousouis, Youssouf El Jarjini, Meryem Touzani, et al.. Geometry, Extent, and Chemistry of Fermentative Hot Spots in Municipal Waste Souk Sebt Landfill, Ouled Nemma, Beni Mellal, Morocco. *Water*, 2024, 16 (6), pp.795. 10.3390/w16060795 . hal-04525846

**HAL Id: hal-04525846**

**<https://hal.science/hal-04525846>**

Submitted on 28 Mar 2024

**HAL** is a multi-disciplinary open access archive for the deposit and dissemination of scientific research documents, whether they are published or not. The documents may come from teaching and research institutions in France or abroad, or from public or private research centers.

L'archive ouverte pluridisciplinaire **HAL**, est destinée au dépôt et à la diffusion de documents scientifiques de niveau recherche, publiés ou non, émanant des établissements d'enseignement et de recherche français ou étrangers, des laboratoires publics ou privés.



Distributed under a Creative Commons Attribution 4.0 International License

## Article

# Geometry, Extent, and Chemistry of Fermentative Hot Spots in Municipal Waste Souk Sebt Landfill, Ouled Nemma, Beni Mellal, Morocco

Yousra El Mouine <sup>1,2</sup>, Amal El Hamdi <sup>1,2</sup> , Abderrahim Bousouis <sup>3</sup>, Youssouf El Jarjini <sup>2</sup> , Meryem Touzani <sup>4</sup>, Vincent Valles <sup>1</sup> , Laurent Barbiero <sup>5,\*</sup>  and Moad Morarech <sup>2</sup>

- <sup>1</sup> Laboratory Mediterranean Environment and Agro-Hydrosystem Modelling (UMR 1114 EMMAH), Hydrogeology Department, Avignon University, 84000 Avignon, France; yousra.elmouine@gmail.com (Y.E.M.); amalgoaea@gmail.com (A.E.H.); vincent.valles@outlook.fr (V.V.)
- <sup>2</sup> Laboratory in Applied and Marine Geosciences, Geotechnics and Georisk (LR3G), Faculty of Science Tetouan, Abdelmalek Essaâdi University, Tetouan 93002, Morocco; youssouf.eljarjini@etu.uae.ac.ma (Y.E.J.); mmorarech@uae.ac.ma (M.M.)
- <sup>3</sup> Laboratoire de Géosciences, Faculté des Sciences, Université Ibn Tofaïl, BP 133, Kénitra 14000, Morocco; ab-derrahim.bousouis@uit.ac.ma
- <sup>4</sup> National Institute of Agronomic Research, Rabat 10060, Morocco; meryem.touzani@inra.ma
- <sup>5</sup> Institut de Recherche pour le Développement, Géoscience Environnement Toulouse, CNRS, University of Toulouse, Observatoire Midi-Pyrénées, UMR 5563, 14 Avenue Edouard Belin, 31400 Toulouse, France
- \* Correspondence: laurent.barbiero@get.omp.eu

**Abstract:** The presence of fermentative hotspots in municipal waste dumps has been reported for several decades, but no study has focused on their size and shape. The uncontrolled landfill of Soub Sekt, covering an area of about 8 hectares in the Tadla plain in Morocco, is the source of a permanent pollution plume in the groundwater, detected by self-potential (SP) measurements. The study aims to detect and characterize these hotspots as well as the leachates that form within them. These hotspots are typically circular and smaller than 3 m in size, and they are concentrated within recent waste deposits. Intense electron transfer activities, particularly during redox reactions leading to metal solubilization, result in very low SP values (down to  $-60$  mV), facilitating their detection. Several successive field campaigns suggest that they are active for 2–3 weeks. Due to the low permeability of the soils, highly mineralized leachates (average Electrical Conductivity  $45$  mS  $\text{cm}^{-1}$ ) rich in organic ions accumulate on the soil surface at the base of the waste windrows. There, they evolve by concentration due to evaporation and oxidation due to slow diffusion of atmospheric  $\text{O}_2$ . Despite the small size of the hotspots generating the leachates, the accumulation of leachates in ponds and the low soil permeability limits the percolation rate, resulting in moderate but permanent groundwater pollution.

**Keywords:** self-potential; redox potential; leachate plume; landfill; Tadla; Morocco



**Citation:** El Mouine, Y.; El Hamdi, A.; Bousouis, A.; El Jarjini, Y.; Touzani, M.; Valles, V.; Barbiero, L.; Morarech, M. Geometry, Extent, and Chemistry of Fermentative Hot Spots in Municipal Waste Souk Sebt Landfill, Ouled Nemma, Beni Mellal, Morocco. *Water* **2024**, *16*, 795. <https://doi.org/10.3390/w16060795>

Academic Editor: Ruben Miranda

Received: 18 February 2024

Revised: 1 March 2024

Accepted: 5 March 2024

Published: 7 March 2024



**Copyright:** © 2024 by the authors. Licensee MDPI, Basel, Switzerland. This article is an open access article distributed under the terms and conditions of the Creative Commons Attribution (CC BY) license (<https://creativecommons.org/licenses/by/4.0/>).

## 1. Introduction

Municipal waste landfills, true biological reactors, are the scene of fermentative processes closely linked to temperature, the nature of the waste, as well as the level of organic matter and moisture, the latter varying due to numerous factors such as climate, cultural and dietary norms, and the possible presence of waste selective sorting [1]. Municipal waste landfills also stand out due to a strong heterogeneity of deposited materials, varying according to their nature, water content, and the proportion of fermentable compounds [2]. The succession of deposits over time maintains this heterogeneity in the intensity of fermentative processes, depending on whether the deposit is recent and rich in fermentable compounds or old and has already undergone these processes. Furthermore, waste decomposition leads to the production of gas and leachate, as well as heat generation, due to

continuous aerobic and anaerobic processes [3]. Although a wild landfill can generally be considered an anaerobic reactor, where organic matter degradation occurs, the composition of the leachates generated, which can contaminate groundwater resources due to their infiltration, varies considerably depending on the location [4–6].

Geophysical methods employing non-invasive approaches are highly adept at mapping the scope of fermentative activities. Among various geophysical methodologies, self-potential (SP) measurements have been applied for approximately three decades in research concerning landfill pollution [7–9]. In recent years, there has been a surge in research focusing on contamination, attributed to the remarkable sensitivity of self-potential measurements to redox conditions in shallow aquifers [10–13]. Notably, the detectable self-potential observed at the surface of the soil is responsive to spatial fluctuations in charge flux within the matrix, variations in redox gradients and temperature, signals generated by microorganisms, or other activities associated with the migration of contaminants [7,12,14–17]. Mapping of fermentative activity in a European landfill using the self-potential (SP) technique has highlighted the existence of “hot spots”, areas subject to intense fermentative processes under the control of microbial activities and geochemical reactions [9,18]. These phenomena, often studied in soil, intensify with the abundance of organic matter and aeration conditions. Fermentative processes there are intense, generating long-term heat, notably through gas escape, such as methane, which can spontaneously ignite [19]. Few studies have focused on these hot spots, with most merely mentioning their existence [18]. Are they present in all operating municipal waste landfills and distributed randomly or concentrated within recent waste? Analysis of these specific areas could provide crucial information to monitor landfill activities and estimate the location of unauthorized or unlisted landfills. The self-potential method has also been used outside landfills [20–23] to map pollution plumes in aquifers resulting from the arrival of leachates from landfill fermentations. These studies have also confirmed the existence of hot spots through very negative values, explained by the intensity of biogeochemical processes.

This study aims to verify the presence and locate fermentative hot spots within a landfill based on the type and approximate age of the waste. It also aims to characterize the shape, size, and spatial variability of fermentative “hot spots” that can cause aquifer contamination, as well as the chemical composition of the leachates they produce, with a focus on the specific conditions of hot and arid zones in North Africa.

## 2. Materials and Methods

### 2.1. Study Area

The study was conducted at the Souk-Sebt Ouled Nemma landfill, an uncontrolled and unsupervised landfill for which no measures have been taken to limit its impact on the environment. It covers approximately 8 hectares in the Tadla plain, the main agricultural production region of Morocco (Figure 1). The site is located on the left bank of the Oum Er Rbia river, which traverses the plain from east to west. The groundwater level, situated approximately 5–6 m beneath a hardened limestone crust, flows in a regional direction towards the north-northwest [24]. The climate in this area is semi-arid to arid continental, characterized by a dry season spanning from April to October and a wet season from November to March. The average yearly temperature hovers around 20 °C, with an annual precipitation average of about 430 mm [25]. The Tadla plain receives water from the Atlas Mountains to the south. Apart from this natural water source, an extensive irrigation system was established in the late 1990s, drawing water from the Bin El Ouidane dam, situated roughly 100 km upstream from the region. This irrigation network is aging; it has numerous leaks that contribute locally to groundwater recharge, causing fluctuations in groundwater levels during irrigation periods. Surface soils in the region have fine textures and moderate permeability. There are many unauthorized landfills within the plain [26]. The Souk-Sebt landfill is surrounded by agricultural plots generally irrigated from late April to late June. The soil in the landfill, compacted by the weight of trucks dumping waste, is rather impermeable, and the leachate produced infiltrates very slowly. During

winter, although rainfall is not abundant, it is sufficient to generate leachate pools within the landfill, each reaching up to 1 m in depth and extending over several tens of square meters [22].

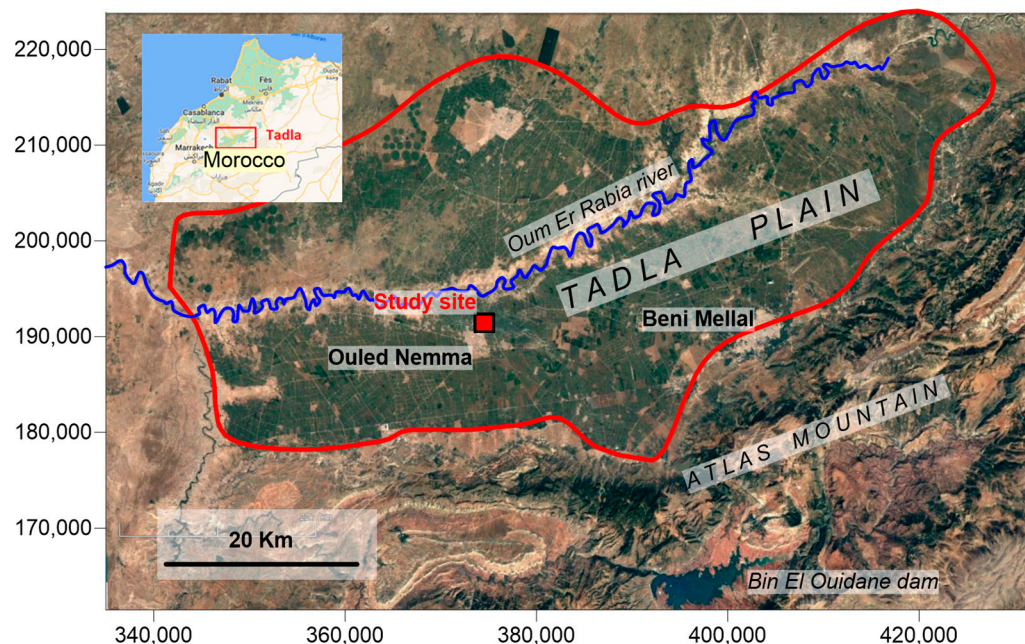


**Figure 1.** Location of the study site on the left bank of the Oum Er Rabia river, Tadla plain, Morocco.

## 2.2. Soub Sekt Landfill

The Soub Sekt landfill, located north of the town of Ouled Nemma, primarily receives household and agricultural waste, but more recently, organic residues from a confectionery factory have been regularly dumped there. Active since the 2000s, the landfill receives regular inputs of materials deposited in windrows. The oldest waste is typically at the base of the windrows (Figure 2a). However, after several years, the waste covers almost the entire surface. Remodeling of old waste is therefore regularly carried out to free up space for new waste and maintain access for dump trucks. This results in areas of accumulation of old materials and areas of recent deposits. Notably, there is a sector of old waste mixed with construction materials, a sector of old deposits in overlapping windrows, and a sector of recent waste deposition. This morphology changes little, but the quantity of added deposits varies over time. Thus, the northeast of the landfill has proven to be a very active sector in terms of fermentative processes. This landfill is the source of a pollution plume that remains stable throughout the season, flowing towards the north-northwest, consistent with our understanding of the regional groundwater flow. The plume, continuously fed by leachates infiltrating beneath the landfill, was detected through PS measurements and sampling during a previous study [22] (Figure 2b). The rapid flow of the groundwater suggests pollution over a long distance, although it has not been mapped in detail. The concerning aspect of the groundwater quality's deterioration is heightened by the fact that rural communities in this area rely directly on aquifer pumping for their water needs, given the isolation of their residences.



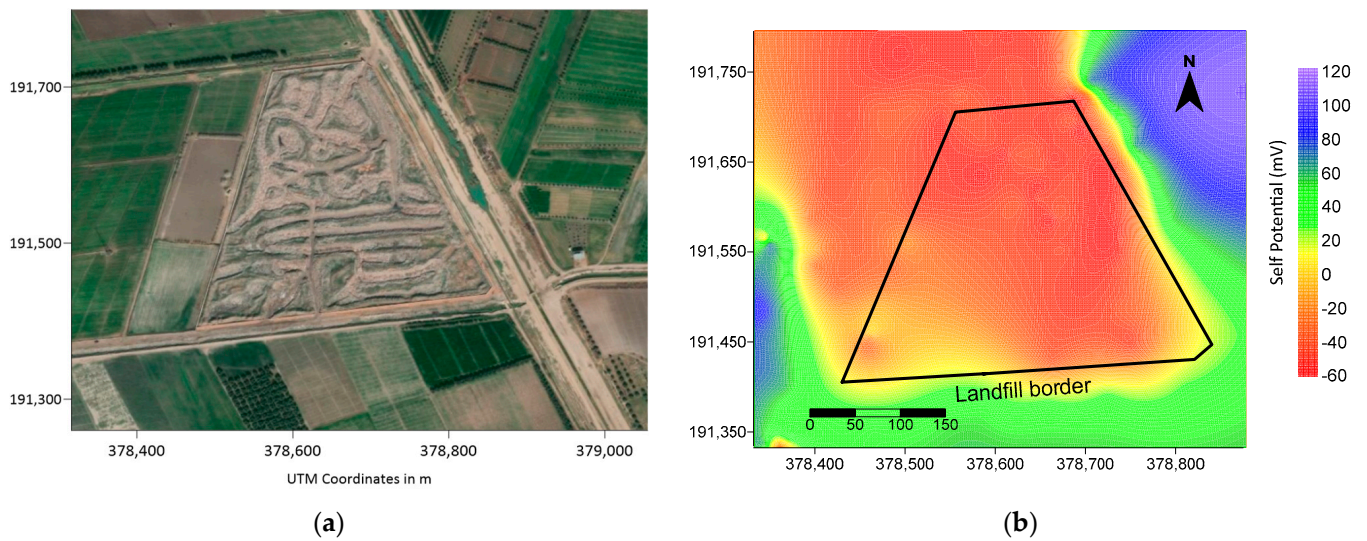


**Figure 2.** (a) Aerial view of the Soub Sekt landfill site showing windrow deposits of waste; (b) pollution plume generated by the Soub Sekt landfill detected from self-potential measurements (adapted from El Mouine et al. [22]).

### 2.3. Self-Potential Measurements

The self-potential measurements were carried out using impolarizable electrodes of type PMS 9000: Pb-PbCl<sub>2</sub> NaCl from SDEC France. These probes have an internal resistance of 450 Ohms. They are sealed with porous wood, and an electrolytic solution of NaCl ensures electrical continuity between the inside of the electrode and the soil. The connections are made with multi-stranded copper cable with a section of 0.75 mm<sup>2</sup> surrounded by plastic insulation. The voltmeter used (Widewing Multimeter UNIT-T 71-C, Petiau type, SDEC, Rousset, France) has a high input impedance (40 MΩ) for reliable measurement. An electrode was installed at a fixed point outside the landfill, defining the baseline potential. The second electrode was moved over the landfill. For each measurement of potential difference, the position of the mobile electrode was measured by GPS and noted. The surface of the landfill and its immediate external environment were swept to promote contact with the ground. The measurement is noted when the measured potential is stabilized, i.e., when the voltage fluctuations do not exceed 2 mV. Due to the irregularity of the terrain, the measurements were not carried out according to a strict grid but rather to cover the area substantially based on obstacles, with particular attention to the north of the landfill identified as more reactive from a fermentative standpoint. Curved lines of measurements were followed with a measurement taken every 5 m along these lines. Measurements were thus sometimes taken between two windrows, sometimes at the top or on the sides of the windrows. Measurements were also taken around the perimeter of the landfill. When a hot spot was detected by a low value of electrical potential, the mobile electrode was moved to detect its center associated with the minimum value. From this position, a series of measurements was taken in a star pattern in 8 directions (North, South, East, West, Northeast, Southeast, Southwest, Northwest) and at intervals of 0.5 m (0.5, 1, 1.5, and 2 m). Each hot spot was thus characterized by 33 SP measurements (Figure 3). Some hotspots, which may be close to each other with overlapping zones of influence on PS measurements, were not studied; only isolated hotspots were considered.

### 2.4. SP Data Treatment

The variograms were calculated and fitted with a model including the nugget effect and a spherical adjustment. Raw and directional variograms were examined to (1) verify if the measurement density is sufficient for a good cartographic representation of SP values on the landfill and (2) detect any potential anisotropy or oriented structure of the values. Maps were generated using kriging (Surfer19, Golden Software, [www.goldensoftware.com](http://www.goldensoftware.com)).

For the study of size and shape, 8 hot spots were selected. The center of each was placed at coordinate (0, 0) and assigned a zero potential value (0 mV) to standardize, allowing for the overlay and comparison of measurements taken in a star pattern. The deviations from the center thus enable the calculation of means and standard deviations in different directions. Therefore, 264 measurements were used for geostatistical processing of data regarding the size and shape of the hot spots.

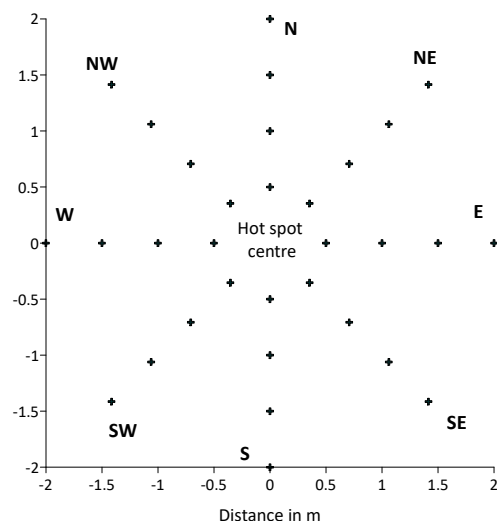
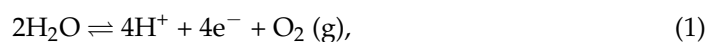


**Figure 3.** Star SP measurements around the center of fermentative hotspots.

### 2.5. Leachates Sampling and Analysis

Seven leachate samples were taken near hotspots in the area of recent deposits, as well as towards the center of the landfill and in the sector occupied by older deposits. Leachates are thick, typically odorous liquids, usually black in color but sometimes red or white. In the deepest ponds (0.7 to 1.1 m), a gradient of physico-chemical characteristics between the surface and depth has been observed. We also noted the presence of a layer of floating plastic waste that significantly reduces the exchange surface between the liquid leachate and the atmosphere. Samples were collected at the surface and at depths of around 0.7 m for the deepest ponds. Electrical conductivity, pH, redox potential (Eh), and temperature were measured on-site. The equipment used is a Hanna Instrument HI98150 pH-meter (Hanna Instrument, Lingolsheim, France). The redox electrode is a platinum electrode with a half-cell KCl/AgCl<sub>2</sub>. The potential of the half-cell, which depends on temperature, was added to the voltmeter reading to obtain the redox potential Eh. These field-acquired data were used to calculate the partial pressure of O<sub>2</sub> according to the formula:



This reaction, having slow kinetics, results in thermodynamic imbalance [27]. Calculating the equilibrating partial pressure of O<sub>2</sub> offers the advantage of combining pH and Eh measurements to estimate an overall parameter of anoxia, i.e., the logarithm of O<sub>2</sub> partial pressure (pO<sub>2</sub>).

Samples were collected in 250 mL HDPE bottles with double closure and without air bubbles. Due to the substantial stock of organic matter in the bottle, microbial activity consuming oxidants is maintained between sampling and laboratory analysis. The samples were transferred to the laboratory (Emmah, Avignon University, France) for analysis of total organic carbon (TOC) by combustion, then, after dilution and filtration to 0.45 μm (cellulose acetate syringe filters), analysis of major anions and cations by ion chromatography and metals by atomic adsorption. Stable isotope analysis of water was conducted on three remaining samples on a Los Gatos Isotope Ratio Infrared Spectrometer (IRIS) (LGR DLT-100, Los Gatos Research Inc., Los Gatos, CA, USA) at the University of Avignon (Accuracy

$\pm 0.2\%$  vs. V-SMOW for  $\delta^{18}\text{O}$  and  $\pm 1\%$  vs. V-SMOW for  $\delta^2\text{H}$ ). These samples were then sent to ENSCM Laboratory (National High School of Chemistry, Montpellier, France) for analysis of trace elements by ICP-MS. Although these 3 samples are not representative of all the processes occurring in the landfill, principal component analysis was conducted to highlight the main evolutions of leachates within the landfill (XLStat software, addinsoft, <https://www.xlstat.com>).

### 3. Results

#### 3.1. Self-Potential Survey of the Landfill Site

The locations of PS measurement points are depicted in Figure 4a. The variogram obtained over the entire landfill is shown in Figure 4b. The spatial structure exhibited a very strong nugget effect, approximately half of the sill. This indicates high variability at the local scale due to the presence of very small hotspots with highly negative values, much smaller than the 5 m distance maintained between successive measurements. Consequently, the distribution map of values (Figure 4a) only reflects the collected data but does not adequately represent the structure of PS values on the study area surface. Based on this result, the exploitation of directional variograms was not meaningful. The map only reflects general trends, with values mostly positive (from  $-5$  to  $+15$  mV) in the extreme southeast of the landfill, composed of older deposits mixed with construction rubble. The southwest third of the landfill was characterized by weakly negative values (from  $-5$  to  $-30$  mV), although some hotspots may be detected there. This sector consists of older waste onto which some recent deposits (around one to two weeks before the measurement campaign) have been accumulated. The northern part of the landfill, as well as a strip along the truck access in the southern part, showed more strongly negative values (from  $-30$  to  $-60$  mV) and are mainly characterized by the concentration of recent deposits. The map highlights the presence of numerous hotspots throughout the landfill, sometimes very close to each other in the northern sector. Several campaigns conducted a few months apart showed that this zoning of the landfill is relatively constant, but the location of hotspots constantly changes depending on the deposits.

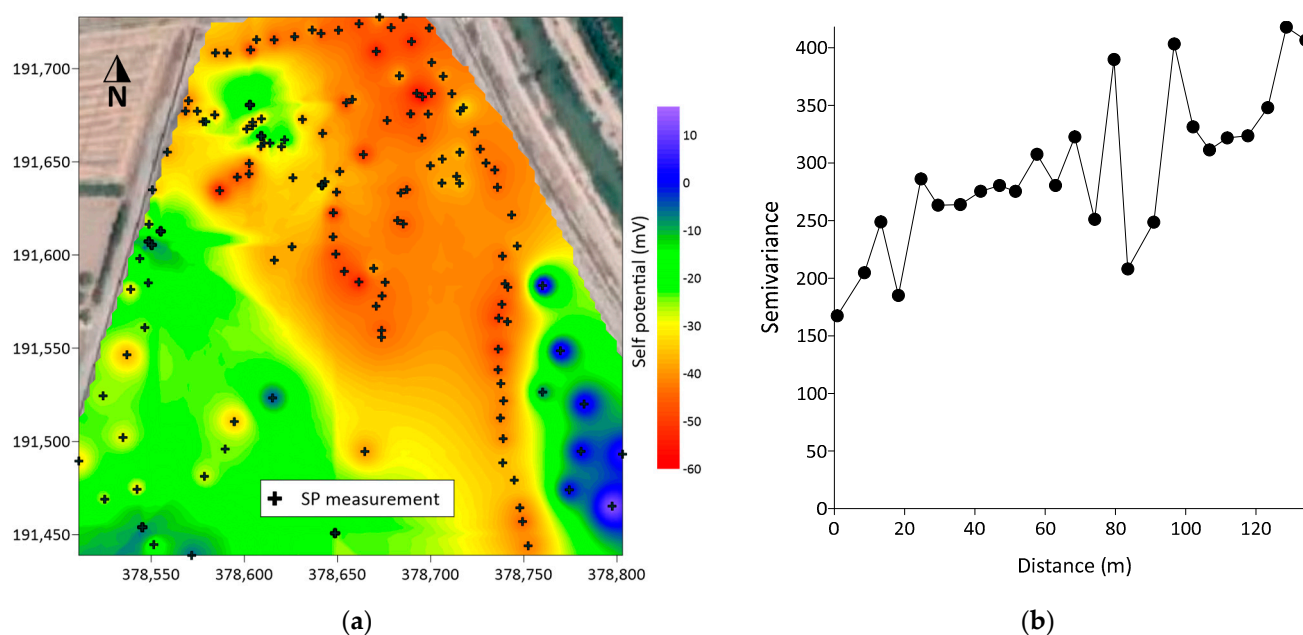


**Figure 4.** Distribution map (a) and variogram (b) of PS values within the landfill.

#### 3.2. Size and Shape of Fermentative Hotspots

In Figure 5a, the color scale has been adapted to highlight abrupt variations in PS around hotspots in accordance with the nugget effect observed on the variogram (Figure 4b).

Hotspots were characterized by very negative PS values (from  $-40$  to  $-60$  mV) but were sporadic. The means and standard deviations of PS values in the measured directions around hotspots are presented in Figure 6, along with the corresponding variogram in Figure 5b. There was an absence of nugget effect with low semivariance for distances less than  $0.4$  m. Semivariance increased very rapidly for distances from around  $1$  to  $1.6$  m, then decreased abruptly for distances greater than  $2.5$  m, indicating a strong structuring of the analyzed environment, with a structure close to  $2.5$  m. The results confirmed the small size of these hotspots, around  $2.5$ – $3$  m in diameter, in accordance with the significant nugget effect observed in Figure 4b at the scale of the landfill. Beyond a distance of  $1.5$  m from the center, the hotspot is no longer detectable. The same aspect was observed in all directions, with slight variations in terms of potential differences from the center (Figure 6).

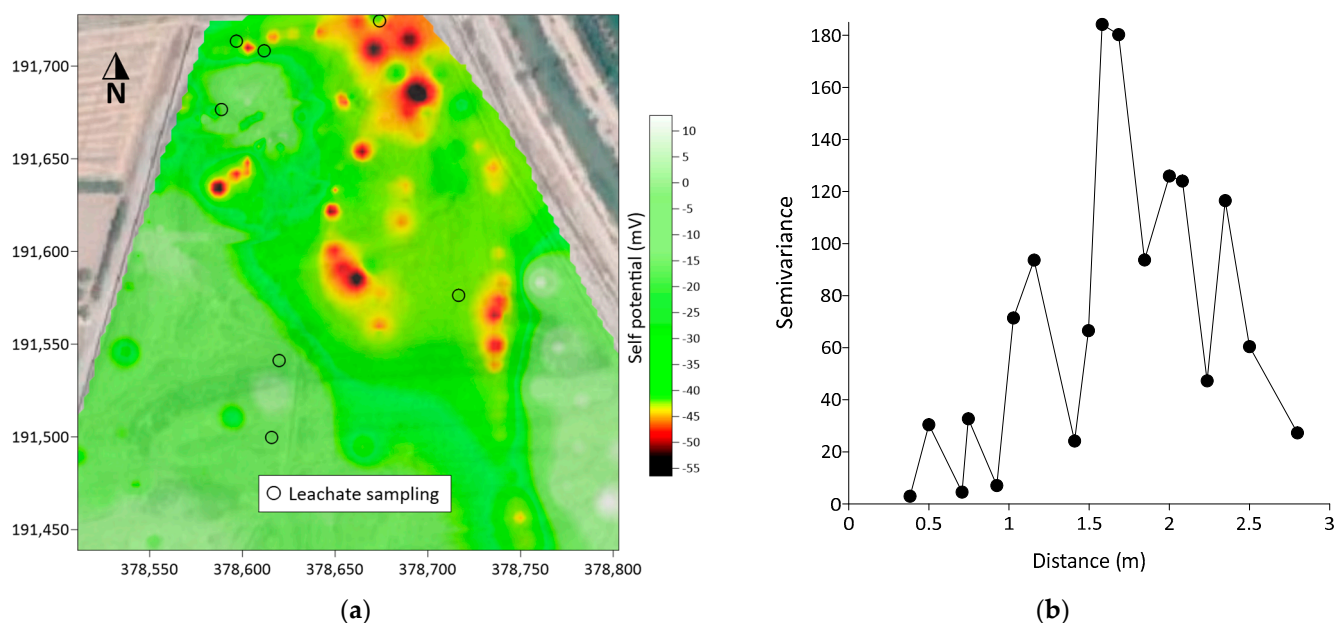


**Figure 5.** (a) Distribution of fermentative hotspots mainly in the northern part of the landfill and leachate sampling; (b) variogram of self-potential measurements around hotspots (average over 8 hotspots).

A mean shape can be established from the 8 cases studied (Figure 7), confirming that the hotspots are nearly circular without any preferential orientation. This shape reflects the projection of a sphere onto the surface of the stacked deposits. The fermentative mass is thus punctual or spherical, without elongation in any preferred direction.

### 3.3. Leachates Characteristics

The leachates were all highly mineralized with an average electrical conductivity of  $45 \text{ mS cm}^{-1}$ . There was a noted disparity between the sum of major ions and electrical conductivity, which is typically around  $1 \text{ mmol}_c$  per  $50 \text{ }\mu\text{S cm}^{-1}$ , for waters in natural environments, whereas, in the case of leachates, it averaged  $1 \text{ mmol}_c$  per  $200 \text{ }\mu\text{S cm}^{-1}$ . The pH was generally neutral, ranging from 6.02 (surface black leachate) to 8.35 (white leachate). The calculated partial pressure of  $\text{O}_2$  ranged from  $10^{-63}$  to  $10^{-50}$  atm. The levels of organic carbon, major ions, and trace elements were very high (Table S1). PCA conducted on all parameters revealed two major processes: mineralization (Principal Component F1) and redox processes (Principal Component F2, Table 1). The coefficients of the parameters electrical conductivity (EC) and redox potential (Eh) showed a negative correlation, with the most concentrated leachates being generally the least reducing.



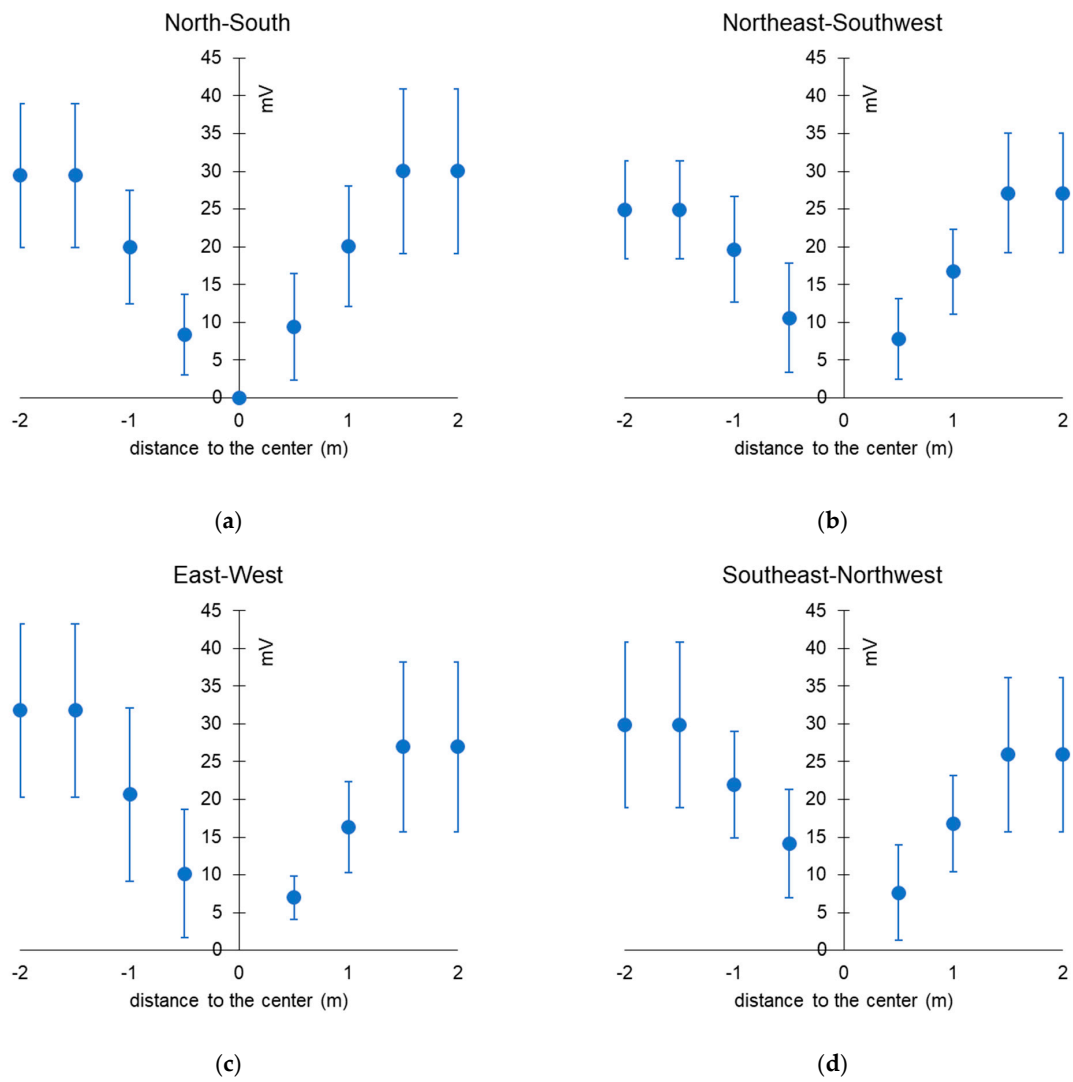


**Figure 6.** Averages and standard deviations of PS variations for hot spots in the (a) north-south, (b) north-east-south-west, (c) east-west, and (d) south-east-north-west directions around the center.

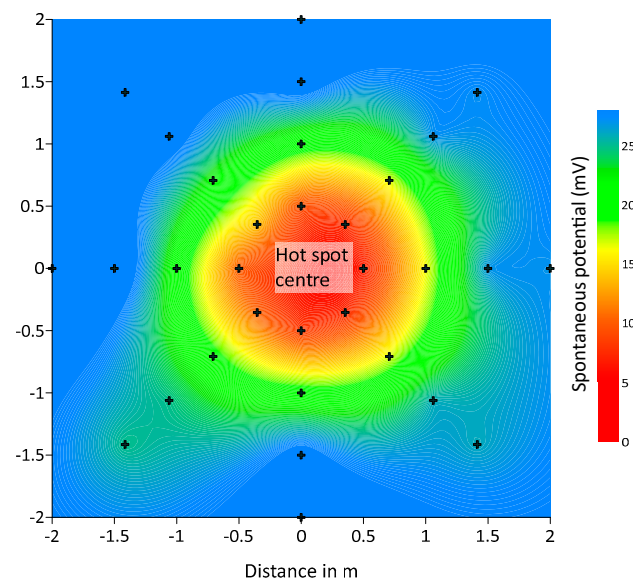


**Figure 7.** Size and shape based on an average of 8 hotspots.

**Table 1.** Coordinates of the various parameters on the first two axes of PCA. Note the coordinates of EC on axis F1 and of Eh on axis F2 (values in bold).

Parameter	F1	F2	Parameter	F1	F2	Parameter	F1	F2
Li	1.00	0.01	Zn	1.00	0.06	F <sup>-</sup>	1.00	-0.03
B	1.00	-0.01	As	0.94	0.33	Cl <sup>-</sup>	0.99	0.16
Na	1.00	0.05	Rb	1.00	0.04	NO <sub>2</sub> <sup>-</sup>	0.99	-0.14
Mg	1.00	-0.06	Sr	0.99	-0.10	Br <sup>-</sup>	0.96	0.27
Al	0.53	0.85	Y	0.99	0.11	NO <sub>3</sub> <sup>-</sup>	0.85	0.53
S	1.00	-0.07	Mo	-0.10	-0.99	SO <sub>4</sub> <sup>2-</sup>	1.00	-0.09
K	1.00	0.05	Cd	0.81	-0.58	Na <sup>+</sup>	0.99	0.15
Ca	0.99	-0.10	Sb	1.00	-0.02	NH <sub>4</sub> <sup>+</sup>	1.00	0.05
Ti	-0.02	1.00	Cs	1.00	0.06	K <sup>+</sup>	0.99	0.13
V	0.99	0.16	Ba	1.00	-0.05	Mg <sup>2+</sup>	1.00	-0.07
Cr	0.52	0.85	Tl	-0.99	0.17	Ca <sup>2+</sup>	0.99	-0.16
Mn	0.99	-0.16	Pb	0.95	0.32	SiO <sub>2</sub>	-0.04	-1.00
Fe	0.99	-0.16	U	0.89	-0.46	pH	-0.61	0.79
Co	1.00	0.05	EC	0.90	0.43	T °C	0.85	-0.52
Ni	1.00	0.05	HCO <sub>3</sub> <sup>-</sup>	1.00	-0.04	Eh	0.32	-0.95
Cu	1.00	0.10	TOC	0.85	-0.52			

All samples exhibited highly reducing characteristics. Yet, the observed classification of leachates seems to align with varying levels of reduction, as red or white leachates exhibit lower reducing values compared to black leachates. The latter, which are the most common in the field, exhibited marked stratification of Eh-pH parameters within the ponds. Pourbaix diagrams (Eh-pH) were plotted for nitrogen, iron, sulfur, and carbon (Figure 8).

Deep leachates were close to the domain of methane production, consistent with the observed spontaneous combustion fumaroles on-site. All samples were in the domain of ammoniacal nitrogen, explaining the presence of NH<sub>4</sub><sup>+</sup> in the laboratory-analyzed samples, unlike NO<sub>3</sub><sup>-</sup>, which appeared only exceptionally, probably due to slight nitrification during the transportation of some samples. All samples were also in the domain of soluble ferrous iron, explaining the abundance of Fe observed in the leachate analysis. The leachates were close to the iso-activity limit of sulfate-sulfide, a theoretical equilibrium difficult to achieve because sulfides are insoluble and precipitate as they form. This transformation from sulfate to sulfide always occurs above the theoretical line of activity equality, as observed for deep black leachates.

Regarding the isotopic signature of the leachates, two out of the three analyzed samples were close to the local meteoric water line [28], while the third deviated significantly, indicating an evaporation process (Figure 9). This sample also showed partial oxidation on the Pourbaix diagrams.

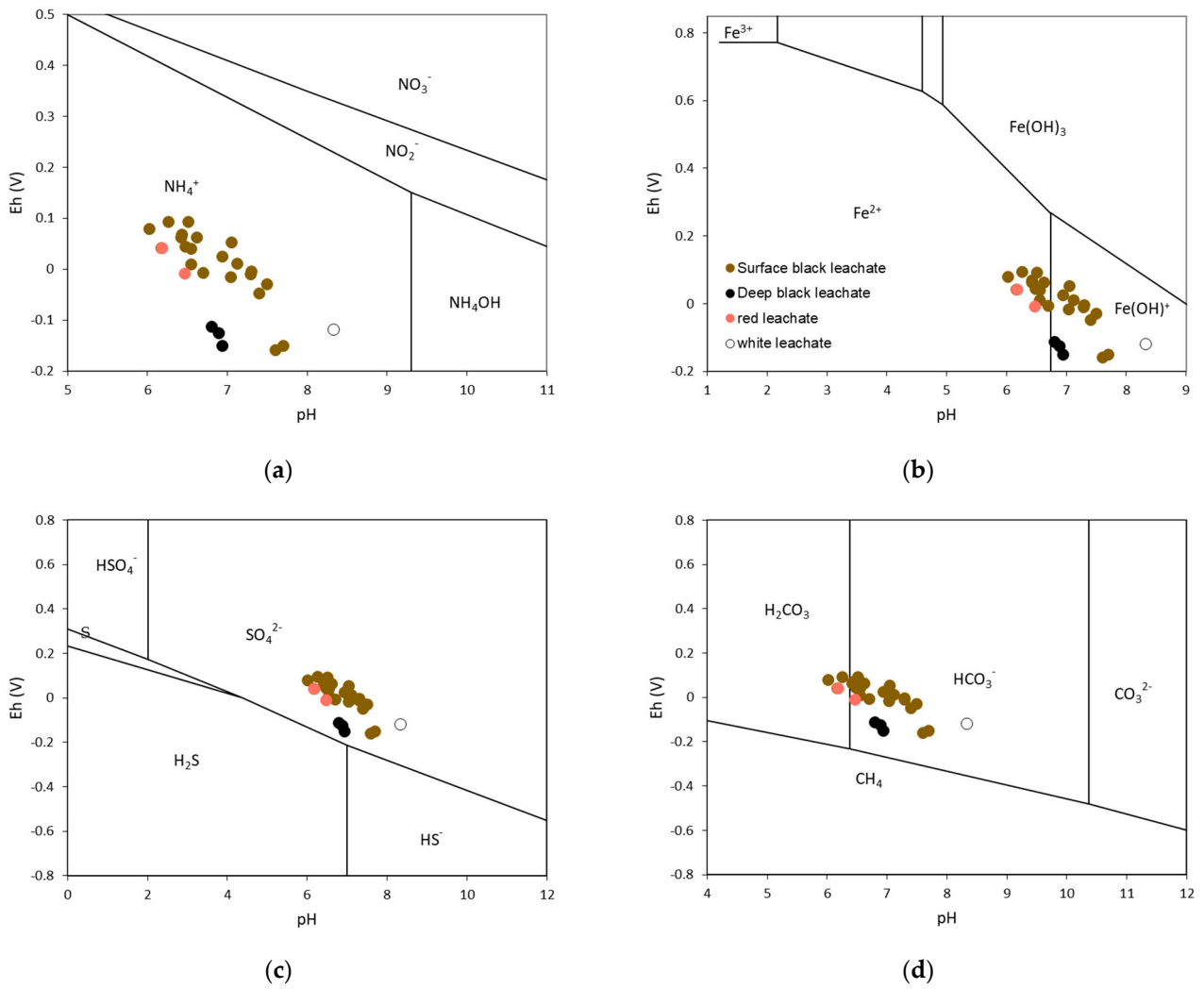


**Figure 8.** Pourbaix diagram showing the species stability domains of leachates for (a) N, (b) Fe, (c) S, and (d) C.

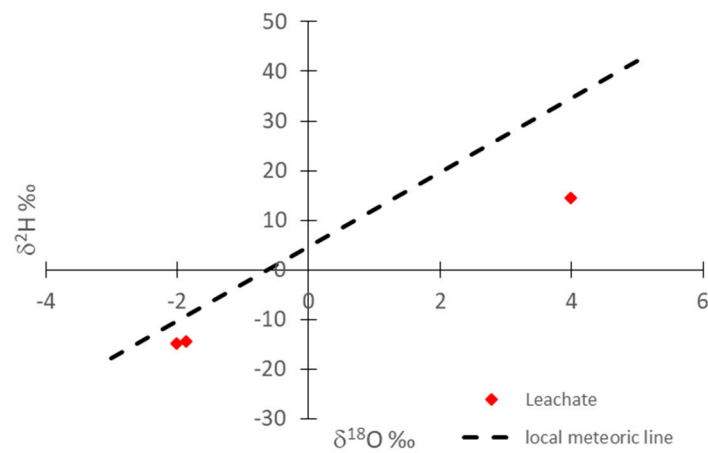


**Figure 9.** Stable isotopic signature of the leachate and its location with respect to the local meteoric line [28].

## 4. Discussion

### 4.1. Intermittent and Fleeting Fermentation Processes

The previous study conducted on the detection and characterization of pollution plumes originating from the Soub Sekt landfill highlighted relatively moderate contamination, mainly due to dilution by leaks from the irrigation network, but persistent throughout the year [22]. However, leachates are produced at small-scale fermentation hotspots, primarily within recent waste. The presence of fermentation hotspots, meaning the very localized nature of fermentation points dispersed within the waste, has been mentioned by some authors [29] but has not been the subject of specific studies, apart from methane gas production and emission in landfills [30,31]. Because of the discreet and non-general nature of these fermentation points, each one is likely to exhibit different characteristics. This is reflected notably in distinct colors in the produced leachate. As a result, the few samples collected probably do not represent all the processes occurring within the landfill. The diversity of leachate is a direct consequence of the localized nature of fermentation. The operational duration of fermentation hotspots is limited to a few weeks, but the continuous deposition of newer waste sustains continuous production at the landfill scale. Leachate pools that form at the base of the waste windrows, typically ranging from 10 to 100 m<sup>2</sup> and sometimes reaching 1 m in depth, serve as intermediate storage for leachates. The low permeability of soils limits leachate flow towards the water table, all contributing to limited but continuous contamination towards the water table. The isotopic signature of leachates [32] shows that rainwaters are the source of leachate percolation but also that they undergo an evaporation process after reaching the soil surface at the base of the waste windrows.

### 4.2. Intense Fermentation Processes

Leachate samples exhibit high levels of nearly all elements and very high electrical conductivity. From this point of view, leachates are saline. The disparity between the content of inorganic major ions and EC values, the latter being approximately four times higher in relation to the corresponding sum of major ions, confirms that a significant proportion of the leachate ionic load is organic. These compounds have a strong complexing power and promote metal solubilization, which can be facilitated by attack from organic acids on metallic waste [33]. The highly reducing nature of the hotspots favors the transition of metals into their reduced form, which is generally more soluble (with a few exceptions). The very low redox potential values at the core of the hotspots reflect intense electron exchange activity, particularly during redox processes leading to metal solubilization, following the principle of a geobattery [12,18,29,34]. Once metals are solubilized, organo-metallic complexation protects them from subsequent precipitation by oxidation, which is itself delayed by slow oxygen diffusion and the preferential oxidation of easily biodegradable carboxylic acids [35]. Thus, oxidation through atmospheric O<sub>2</sub> diffusion to the liquid phase within the pools primarily oxidizes the most labile forms of organic matter before oxidizing other components. The high organic content acts as a sort of redox buffer, maintaining highly reducing conditions in the leachates over the long term, even after migration from hotspots to pools.

## 5. Conclusions

Our study confirms the presence of fermentation hotspots in the landfill under investigation. These hotspots, small in size and rich in fermentable organic matter, are the site of intense fermentation processes, accompanied by electron exchanges that allow their detection through self-potential measurements. Low potential (SP) values are detectable on the surface of the waste within a maximum radius of 1.5 m from the center of the hotspot. Fermentation processes liquefy organic materials and fractionate organic molecules into simpler and more soluble organic acids. These organic acids massively solubilize metals, especially those with affinities for organic matter (such as copper, lead, etc.). The solubilization of compounds occurs through reduction and organometallic complexation. Rare



rains promote the migration of leachates from hotspots to the soil surface at the base of the waste windrows, diluting the fermentation products somewhat. These rains imprint their isotopic signature on the leachates. Once accumulated in the pools, leachates are subjected to two processes: evaporation due to the aridity of the climate and slow oxidation by oxygen diffusion from the atmosphere to the leachate. This latter process is responsible for vertical variability in redox conditions, with the deepest parts of the leachate pools being more reducing than the interface with the atmosphere. The slow oxidation of leachates by atmospheric O<sub>2</sub>, due to the high stock of organic carbon inducing a “redox buffer” effect, maintains the leachate pools under highly reducing conditions. Evaporation leads to an increase in the concentrations of various components. The results obtained from the Souk Sebt landfill cannot be fully extrapolated to other landfills. The low permeability of the soil, compacted by trucks depositing waste, leads to soil sealing and the accumulation of leachates in large pools, which may not necessarily be observed in all landfills. This situation has allowed for the study of leachates and their evolution as they accumulate in pools, a context that, as mentioned in previous work, results in the presence of a permanent pollution plume oriented northwest, in accordance with the regional flow of the aquifer.

**Supplementary Materials:** The following supporting information can be downloaded at: <https://www.mdpi.com/article/10.3390/w16060795/s1>, Table S1: Leachates chemistry (ICPMS and Ion chromatography) and physico-chemical field measurements.

**Author Contributions:** Conceptualization, V.V. and M.M.; methodology, V.V., Y.E.M. and M.M.; software, A.E.H., A.B., Y.E.J. and M.T.; validation, Y.E.M. and A.E.H.; formal analysis, Y.E.M. and A.E.H.; investigation, Y.E.M. and A.E.H.; resources, V.V., M.M. and L.B.; data curation, V.V. and L.B.; writing—original draft preparation, V.V., M.T. and Y.E.M.; writing—review and editing, L.B.; visualization, V.V. and L.B.; supervision, V.V. and M.M.; project administration, M.M. and V.V.; funding acquisition, L.B. and M.M. All authors have read and agreed to the published version of the manuscript.

**Funding:** The first two authors benefited from a national doctoral scholarship from the University of Tetouan and support for international mobility of doctoral students from the University of Avignon (Perdiguer Program). This research did not receive any other funding.

**Data Availability Statement:** The data presented in this study are available in Supplementary Materials.

**Acknowledgments:** The authors thank Avignon and Abdelmalek Essaadi universities and the Dean of the National Institute of Agricultural Research. The authors are also grateful to the staff of the Hydrogeology Laboratory of Avignon for their help and support.

**Conflicts of Interest:** The authors declare no conflicts of interest. The funders had no role in the design of the study; in the collection, analyses, or interpretation of data; in the writing of the manuscript; or in the decision to publish the results.

## References

1. Belevi, H.; Baccini, P. Long-term behavior of municipal solid waste landfills. *Waste Manag. Res.* **1989**, *7*, 43–56. [[CrossRef](#)]
2. Han, Z.; Ma, H.; Shi, G.; He, L.; Wei, L.; Shi, Q. A review of groundwater contamination near municipal solid waste landfill sites in China. *Sci. Total Environ.* **2016**, *569–570*, 1255–1264. [[CrossRef](#)] [[PubMed](#)]
3. Naudet, V.; Revil, A.; Rizzo, E.; Bottero, J.-Y.; Bégassat, P. Groundwater redox conditions and conductivity in a contaminant plume from geoelectrical investigations. *Hydrol. Earth Syst. Sci.* **2004**, *8*, 8–22. [[CrossRef](#)]
4. Jhamnani, B.; Singh, S.K. Groundwater Contamination due to Bhalaswa Landfill Site in New Delhi. *Int. J. Civ. Environ. Eng.* **2009**, *1*, 121–125.
5. Nazli, Y.; Hanson, J.L.; Wei-Lien, L. Heat Generation in Municipal Solid Waste Landfills. *J. Geotech. Geoenvironmental Eng.* **2005**, *131*, 1330–1344.
6. Hanson, J.L.; Yeşiller, N.; Oettle, N.K. Spatial and Temporal Temperature Distributions in Municipal Solid Waste Landfills. *J. Environ. Eng.* **2010**, *136*, 804–814. [[CrossRef](#)]
7. Martínez-Pagán, P.; Jardani, A.; Revil, A.; Haas, A. Self-potential monitoring of a salt plume. *Geophysics* **2010**, *75*, WA17–WA25. [[CrossRef](#)]
8. Revil, A.; Naudet, V.; Nouzaret, J.; Pessel, M. Principles of electrography applied to self-potential electrokinetic sources and hydrogeological applications. *Water Resour. Res.* **2003**, *39*, 1–15. [[CrossRef](#)]

9. Revil, A.; Titov, K.; Doussan, C.; Lapenna, V. Applications of The Self-Potential Method to Hydrological Problems. In *Proceedings of the Applied Hydrogeophysics*; Vereecken, H., Binley, A., Cassiani, G., Revil, A., Titov, K., Eds.; Springer: Dordrecht, The Netherlands, 2006; pp. 255–292.
10. Arisawadi, M. Rahmania Mapping leachate distribution based on the self-potential method in Manggar Landfill, Balikpapan Indonesia. *J. Phys. Conf. Ser.* **2021**, *1763*, 12013. [[CrossRef](#)]
11. Stanly, R.; Yasala, S.; Oliver, D.H.; Nair, N.C.; Emperumal, K.; Subash, A. Hydrochemical appraisal of groundwater quality for drinking and irrigation: A case study in parts of southwest coast of Tamil Nadu, India. *Appl. Water Sci.* **2021**, *11*, 53. [[CrossRef](#)]
12. Arora, T.; Linde, N.; Revil, A.; Castermant, J. Non-intrusive characterization of the redox potential of landfill leachate plumes from self-potential data. *J. Contam. Hydrol.* **2007**, *92*, 274–292. [[CrossRef](#)]
13. Rani, P.; Piegari, E.; Di Maio, R.; Vitagliano, E.; Soupios, P.; Milano, L. Monitoring time evolution of self-potential anomaly sources by a new global optimization approach. Application to organic contaminant transport. *J. Hydrol.* **2019**, *575*, 955–964. [[CrossRef](#)]
14. Gallas, J.D.F.; Taioli, F.; Malagutti Filho, W. Induced polarization, resistivity, and self-potential: A case history of contamination evaluation due to landfill leakage. *Environ. Earth Sci.* **2011**, *63*, 251–261. [[CrossRef](#)]
15. Naudet, V.; Revil, A.; Bottero, J.-Y.; Bégassat, P. Relationship between self-potential (SP) signals and redox conditions in contaminated groundwater. *Geophys. Res. Lett.* **2003**, *30*, 2091. [[CrossRef](#)]
16. Naudet, V.; Gourry, J.C.; Girard, F.; Mathieu, F.; Saada, A. 3D electrical resistivity tomography to locate DNAPL contamination around a housing estate. *Near Surf. Geophys.* **2014**, *12*, 351–360. [[CrossRef](#)]
17. Cui, Y.A.; Liu, L.; Zhu, X. Unscented Kalman filter assimilation of time-lapse self-potential data for monitoring solute transport. *J. Geophys. Eng.* **2017**, *14*, 920–929. [[CrossRef](#)]
18. Revil, A.; Mendonça, C.A.; Atekwana, E.A.; Kulesa, B.; Hubbard, S.S.; Bohlen, K.J. Understanding biogeobatteries: Where geophysics meets microbiology. *J. Geophys. Res. Biogeosciences* **2010**, *115*, G1. [[CrossRef](#)]
19. Artíñano, B.; Gómez-Moreno, F.J.; Díaz, E.; Amato, F.; Pandolfi, M.; Alonso-Blanco, E.; Coz, E.; García-Alonso, S.; Becerril-Valle, M.; Querol, X.; et al. Outdoor and indoor particle characterization from a large and uncontrolled combustion of a tire landfill. *Sci. Total Environ.* **2017**, *593–594*, 543–551. [[CrossRef](#)]
20. Barry, A.A.; Yameogo, S.; Ayach, M.; Jabrane, M.; Tiouiouine, A.; Nakolendousse, S.; Lazar, H.; Filki, A.; Touzani, M.; Mohsine, I. Mapping Contaminant Plume at a Landfill in a Crystalline Basement Terrain in Ouagadougou, Burkina Faso, Using Self-Potential Geophysical Technique. *Water* **2021**, *13*, 1212. [[CrossRef](#)]
21. Touzani, M.; Kacimi, I.; Kassou, N.; Morarech, M.; Bahaj, T.; Valles, V.; Barbiero, L.; Yameogo, S. El impacto del vertedero de Oum Azza sobre la calidad de las aguas subterráneas de Rabat (Marruecos). *Cuad. Geográficos* **2019**, *58*, 68–82. [[CrossRef](#)]
22. El Mouine, Y.; El Hamdi, A.; Morarech, M.; Kacimi, I.; Touzani, M.; Mohsine, I.; Tiouiouine, A.; Ouardi, J.; Zouahri, A.; Yachou, H.; et al. Landfill Pollution Plume Survey in the Moroccan Tadla Using Spontaneous Potential. *Water* **2021**, *13*, 910. [[CrossRef](#)]
23. Touzani, M.; Mohsine, I.; Ouardi, J.; Kacimi, I.; Morarech, M.; El Bahajji, M.H.; Bouramtane, T.; Tiouiouine, A.; Yameogo, S.; El Mahrad, B. Mapping the Pollution Plume Using the Self-Potential Geophysical Method: Case of Oum Azza Landfill, Rabat, Morocco. *Water* **2021**, *13*, 961. [[CrossRef](#)]
24. Massoni, C.; Missante, G.; Beaudet, G.; Combes, M.; Etienne, H.P.; Ionesco, T. La plaine du Tadla. *Cah. Rech. Agron.* **1967**, *24*, 163–194.
25. ABHOER. *Etude D'actualisation du Plan Directeur D'aménagement Intègre des Ressources en eau (PDAIRE) de la zone D'action de L'agence du bassin Hydraulique de l'Oum Er Rbia: Données Générales sur la Plaine du Tadla*; ABHOER: Rabat, Morocco, 2008.
26. Merzouki, H.; Hanine, H.; Lekhlif, B.; Latrache, L.; Mandi, L.; Sinan, M. Physicochemical Characterization of Leachate Discharge Fkih Ben Salah from Morocco. *J. Mater. Environ. Sci.* **2015**, *6*, 1354–1363.
27. Van Loon, G.W.; Duffy, S.J. *Environmental Chemistry: A Global Perspective*, 4th ed.; Oxford University Press: Oxford, UK, 2017.
28. El Ouali, A.; Roubil, A.; Lahrach, A.; Mudry, J.; El Ghali, T.; Qurtobi, M.; El Hafyani, M.; Alitane, A.; El Hmaid, A.; Essahlaoui, A.; et al. Isotopic Characterization of Rainwater for the Development of a Local Meteoric Water Line in an Arid Climate: The Case of the Wadi Ziz Watershed (South-Eastern Morocco). *Water* **2022**, *14*, 779. [[CrossRef](#)]
29. Naudet, V.; Revil, A. A sandbox experiment to investigate bacteria-mediated redox processes on self-potential signals. *Geophys. Res. Lett.* **2005**, *32*, L11405. [[CrossRef](#)]
30. Gonzalez-Valencia, R.; Magana-Rodriguez, F.; Cristóbal, J.; Thalasso, F. Hotspot detection and spatial distribution of methane emissions from landfills by a surface probe method. *Waste Manag.* **2016**, *55*, 299–305. [[CrossRef](#)] [[PubMed](#)]
31. Karimi, N.; Ng, K.T.W.; Richter, A. Prediction of fugitive landfill gas hotspots using a random forest algorithm and Sentinel-2 data. *Sustain. Cities Soc.* **2021**, *73*, 103097. [[CrossRef](#)]
32. Wimmer, B.; Hrad, M.; Huber-Humer, M.; Watzinger, A.; Wyhlidal, S.; Reichenauer, T.G. Stable isotope signatures for characterising the biological stability of landfilled municipal solid waste. *Waste Manag.* **2013**, *33*, 2083–2090. [[CrossRef](#)]
33. Xie, S.; Ma, Y.; Strong, P.J.; Clarke, W.P. Fluctuation of dissolved heavy metal concentrations in the leachate from anaerobic digestion of municipal solid waste in commercial scale landfill bioreactors: The effect of pH and associated mechanisms. *J. Hazard. Mater.* **2015**, *299*, 577–583. [[CrossRef](#)]

34. Rittgers, J.B.; Revil, A.; Karaoulis, M.; Mooney, M.A.; Slater, L.D.; Atekwana, E.A. Self-potential signals generated by the corrosion of buried metallic objects with application to contaminant plumes. *Geophysics* **2013**, *78*, EN65–EN82. [[CrossRef](#)]
35. Ilgen, G.; Glindemann, D.; Herrmann, R.; Hertel, F.; Huang, J.-H. Organometals of tin, lead and mercury compounds in landfill gases and leachates from Bavaria, Germany. *Waste Manag.* **2008**, *28*, 1518–1527. [[CrossRef](#)] [[PubMed](#)]

**Disclaimer/Publisher’s Note:** The statements, opinions and data contained in all publications are solely those of the individual author(s) and contributor(s) and not of MDPI and/or the editor(s). MDPI and/or the editor(s) disclaim responsibility for any injury to people or property resulting from any ideas, methods, instructions or products referred to in the content.